metals

MDPI

Article

Research on the Analysis and Prediction Model of Machining Parameters of Titanium Alloy by Abrasive Belt

Hu Qiao [1], Sibo Hu [1], Ying Xiang [2,*], Shanshan Liu [1] and Li Zhang [1]

[1] School of Mechatronic Engineering, Xi'an Technological University, Xi'an 710021, China; qiaohu@xatu.edu.cn (H.Q.); 13669195655@163.com (S.H.); lss13379436709@163.com (S.L.); 18392657483@163.com (L.Z.)

[2] College of Mechanical and Electrical Engineering, Shaanxi University of Science and Technology, Xi'an 710021, China

* Correspondence: yingcara@hotmail.com

Abstract: As a high-performance and difficult-to-machine material for the manufacture of blades, titanium alloys are increasingly being used in high-end manufacturing industries such as aerospace and aircraft. As engineering applications become more demanding, so do the requirements for precision. However, to date, the choice of blade grinding parameters is still mainly dependent on the traditional "trial cut" and "experience" method, making the processing efficiency low and the quality of processing difficult to be guaranteed. In order to achieve the requirements of high precision and low surface roughness of the workpiece, to get rid of the status quo of relying on manual decision-making, and to achieve reasonable prediction and control of surface quality, this paper proposes to establish a theoretical prediction model for surface roughness of titanium alloy by abrasive belt grinding, and to analyze the influence of the main process parameters on surface roughness during the grinding process through experiments. A theoretical prediction model for surface roughness was developed. The experimental results show that the model has certain accuracy and reliability, and can provide guidance for the high-precision prediction of the surface roughness of ground titanium alloy blades, which has strong practical significance in engineering.

Keywords: titanium alloy; abrasive belt grinding; surface roughness; regression mathematical model

check for updates

Citation: Qiao, H.; Hu, S.; Xiang, Y.; Liu, S.; Zhang, L. Research on the Analysis and Prediction Model of Machining Parameters of Titanium Alloy by Abrasive Belt. *Metals* **2023**, *13*, 1085. https://doi.org/10.3390/met13061085

Academic Editors: Rangappa Suresh and Satish Kumar

Received: 17 April 2023
Revised: 25 May 2023
Accepted: 2 June 2023
Published: 8 June 2023

Copyright: © 2023 by the authors. Licensee MDPI, Basel, Switzerland. This article is an open access article distributed under the terms and conditions of the Creative Commons Attribution (CC BY) license (https://creativecommons.org/licenses/by/4.0/).

1. Introduction

The complex profile structure of the blades is designed to ensure uniform and stable airflow during operation and to reduce energy loss during airflow. This makes the blade different from other irregularly curved parts. Its complex profile brings difficulty to the processing, making it difficult to achieve the ideal machining accuracy, and the surface quality of the workpiece after processing is also difficult to ensure [1].

At present, the manufacturing industry in various countries has similar machining processes for blades, mainly through the combination of milling processing and manual polishing to complete the process. The process includes the use of precision forging or precision casting to produce the blade blank, followed by finishing on a high-precision milling machine, and finally by repeated measurement and manual polishing in combination [2]. This mode of processing is costly, inefficient and does not guarantee the quality of the workpiece. In addition, thin-walled parts are weak and easily deformed. Milling can cause the workpiece or tool to vibrate to a certain extent and, due to the lack of rigidity of the machining system, the cutting forces can also cause the tool to give way, thus causing deformation and affecting the machining accuracy of the part [3]. Therefore, the use of grinding for the machining of blade profiles effectively avoids these problems and guarantees the surface quality of the workpiece. The use of manual grinding is highly dependent on the experience and technical level of the operator, some conventional knowledge and customary experience cannot be applied, and the turnover of processing personnel will also

have a greater impact on the enterprise and the entire processing industry, and excessive reliance on the operator will also put too much pressure on them. Such production methods cannot meet modern production requirements and precision needs, so a new method of processing, to solve the current dilemma, needs to be found.

Current research has found that titanium alloys have some special physical and mechanical properties that make them difficult to grind [4]. Compared with wheel grinding, in abrasive belt grinding the abrasive belt has an elastic state of contact with the workpiece, the abrasive grains have a large squeezing and sliding effect on the surface material of the workpiece, the grinding and polishing effect is strong, and the surface quality of the workpiece is good after processing [5]. Therefore, abrasive belt grinding has an improved processing effect on titanium alloy parts and has been gradually and more widely used. Blade processing for the establishment of a surface roughness prediction model can be based on processing requirements, the process parameters for reasonable settings and appropriate adjustments, so as to obtain the ideal surface to achieve the processing requirements, and can simplify the processing process, and reduce production and processing costs [6–8].

In the grinding of blades, the setting of grinding process parameters plays a decisive role in improving grinding efficiency and workpiece quality. Research results show that surface roughness is one of the important indicators affecting the performance of mechanical parts [9]. The setting of grinding parameters has a great influence on the surface roughness of the blade body and on the internal defects of the blade, which is why the evaluation of surface roughness is of great importance. Many current studies have shown the influence of the grinding process on the surface roughness during grinding [10]. Luo Goshan [11] et al. studied the influence of grinding process parameters on surface roughness and grinding ratio to determine the optimal combination of process parameters. Xiaojun Wu [12] et al. conducted single-factor and orthogonal experimental studies on the grinding grain diameter, grinding speed, depth of cut and feed rate respectively. The experimental results showed that the best grinding quality was achieved at a grit size of 320#, a grinding speed of 4500 r/min, a depth of cut of 0.4 mm and a feed rate of 80 mm/s. Due to the structure and material characteristics of the blade itself, different process parameters, when combined, will produce different effects, which will have a certain impact on the final surface quality and machining efficiency, and will also directly affect the performance of the final product. Zhang Jingjing [13] et al. used single-factor and orthogonal experiments to derive process parameter intervals for better surface roughness during blade blasting and predicted them using a non-linear regression model. Anne Venu Gopal [14] et al. investigated the effects of abrasive belt grit size, depth of cut and feed rate on surface roughness and used ANOVA. The significance of the grinding parameters on the selected response was evaluated. The above evolutionary methods such as GA, ACO, PSO, ABC, etc., used in order to optimize machining process parameters, are widely used in production, but problem solving by these techniques is limited to the inherent search mechanism [15]. In particular, when predicting machining processes, the models perform well for optimization results with a single parameter, but often perform poorly when there are multiple input parameters [16].

For the identification of critical machining parameters to study the surface quality of the blade profile grinding process, predicting the blade surface quality accordingly and adjusting the machining parameters to obtain the desired surface, Prashant J. Patil [17] et al. used G-ratio and surface finish as the objectives, and depth of cut, lubricant type, feed rate, grinding wheel speed, coolant flow rate and nanoparticle size as variables. Chew Ying Nee [18] investigated the effect of rotational speed, feed rate, depth of cut and tool tip arc on surface roughness and used the differential evolution (DE) algorithm to find the combination of process parameters that satisfied the minimum surface roughness. Süleyman Neseli [19] et al. developed two optimization models using computer-aided single-objective optimization methods by combining the surface response method with Taguchi's method, taking into account vibration and surface roughness, and using workpiece speed, feed rate and depth of cut as the objects of study. The experimental results showed that the workpiece speed had the greatest effect on surface roughness and vibration, and the feed

rate had the least effect. Rodrigo de Souza Ruzzi [20] et al. evaluated the effects of several grinding parameters on the surface integrity, grinding force and grinding specific energy of Inconel 625 alloy; partial analysis factor experiments were used to determine the effects of grinding wheel speed, working speed, depth of cut, grinding grain mesh and grinding direction on the surface integrity of Inconel 625 alloy, The surface integrity was evaluated using partial analysis experiments using the grinding wheel speed, working speed, depth of cut, grit mesh and grinding direction as the variables of the grinding process. There are many methods that can be used to make decisions on grinding process parameters, and a number of experts and scholars have conducted corresponding research using case-based reasoning. Gao Wei [21] et al. proposed a case-based variable weight reasoning model for the intelligent optimization of abrasive blocks in drum finishing, using hierarchical analysis to determine the weights of the cases so as to achieve fast and intelligent selection of abrasive blocks in the machining process. fast and intelligent selection of abrasive blocks during machining.

In order to improve the quality of the product, the properties of surface integrity, residual stress, microstructure and mechanical properties were improved [22] and a large number of experiments were required to investigate the inter-relationship between the factors. A comparative study of surface roughness and surface integrity was carried out through experimental analysis, and the results showed that the surface roughness of all ground surfaces conformed to the expected range yielding the optimum machining parameters and thus the optimal process solution [23–25]. Therefore, the selection of the machining parameters and the evaluation of the surface quality are very important in the whole production process. Only a reasonable combination of machining parameters can ensure that the whole process can reach the desired state.

However, most researchers currently study the effect of grinding on surface roughness under single-parameter conditions, and then improve the parameters to adjust surface integrity. The grinding parameters discussed in this paper are divided into abrasive grain size, abrasive belt line speed, grinding pressure, with good contact pressure control, where the test pieces are ground at four combinations of abrasive belt line speed of 10 m/s, 15 m/s, 20 m/s and target pressure of 5 N, 10 N and 15 N, respectively. At the same time, different types of grinding belts were combined at different grinding parameters to derive the expressions of the theoretical model from the test data.

At the same time, in order to achieve a fast selection of parameters in the actual production process, the surface roughness of the workpiece is predicted. On the basis of the above description, this paper presents a study based on the prediction model of surface roughness of titanium alloy in abrasive belt grinding. Firstly, the parameters of the blade in the abrasive belt grinding process are analyzed to determine the key processing parameters in the grinding process with the influence and change laws. Then, a surface roughness prediction model is established to divide the surface roughness into a number of intervals and select the best combination of process parameters for each interval. Finally, the surface roughness can be deduced from the prediction model for each parameter case. It provides a basis for guiding the actual processing, improving the product yield and ensuring the surface quality in the future practical production process [26].

2. Experiment

2.1. Test Materials

The material of the belt grinding specimen is TC4 titanium alloy, which is a type of alloy with the main chemical composition shown in Table 1 below, and its dimensions are: 15 mm × 40 mm (diameter × length) of bar stock. Four types of abrasive belts were used: Chinese TJ113 abrasive belts with an aluminum oxide grain size of 80# and 150#; 3M™ Trizact™ (3M Company, St. Paul, MN, USA) abrasive belts with an aluminum oxide grain size of A35 (600#) and A160 (120#), with a belt width of W = 25 mm; and a belt circumference of L = 1510 mm.

Table 1. Main Chemical Composition of Titanium Alloy.

Element	Ti	Al	V	O	Fe	C
Components (at.%)	89.239	6.170	4.230	0.160	0.150	0.030

2.2. Test Platform and Conditions

The design and construction of an abrasive belt model test bench capable of performing grinding experiments at constant pressure and constant linear speed is based on the need to study the surface roughness of titanium alloy materials by abrasive belt grinding. The designed abrasive belt grinding test bench is shown in Figure 1 below.

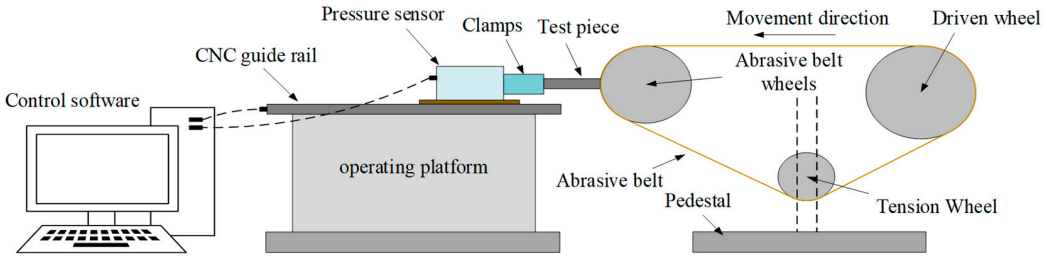


Figure 1. Belt grinding experiment platform.

The belt grinding experiment platform consists of a belt with adjustable speed, a clamping device, a pressure sensor and a CNC guide rail driven by a stepper motor. The quadrangular chuck connected to the pressure sensor can hold a test piece with a square cross-section close to and in contact with the belt for grinding [27]. The pressure sensor measures the pressure between the test piece and the contact wheel in real time and feeds it back to the control software. The control software compares the measured pressure with the pre-set target pressure and controls the NC guideway to move forward or backward at a certain speed according to the deviation between the two, thus keeping the contact pressure between the test piece and the contact wheel constant.

2.3. Control Software for the Constant Force Abrasive Belt Experiment Platform

In order to realize constant force belt grinding, the belt grinding experiment platform built in this paper is controlled by the PID (proportion integral differential) algorithm [28]. As one of the most widely used algorithms in continuous systems, the PID control algorithm has the advantages of simplicity and efficiency, and can work in various non-linear and time-varying environments [29]. The PID control algorithm integrates the functions of proportional, integral and differential links, and its scope of application is the case where the object designation in the controlled model is unclear. According to theoretical analysis and experimental research results, the model has good adaptability to complex and variable problems, where it is not easy to establish an accurate mathematical model, where it is difficult to obtain an optimal solution with traditional PID algorithms, and where automation can be achieved. In essence, the PID algorithm is a control structure based on feedback correction of the error signal, adaptively adjusting the parameters to bring them to the desired value, so as to obtain a closed-loop controller that meets the requirements, and outputting the calculation results in the form of control signals to the actuators, so that they can complete the task of executing the instructions or commands, and through iterative operations the error of the system can be limited to a given range to ensure the control accuracy and stability of the system [30]. The principle of the PID control algorithm is shown in Figure 2.

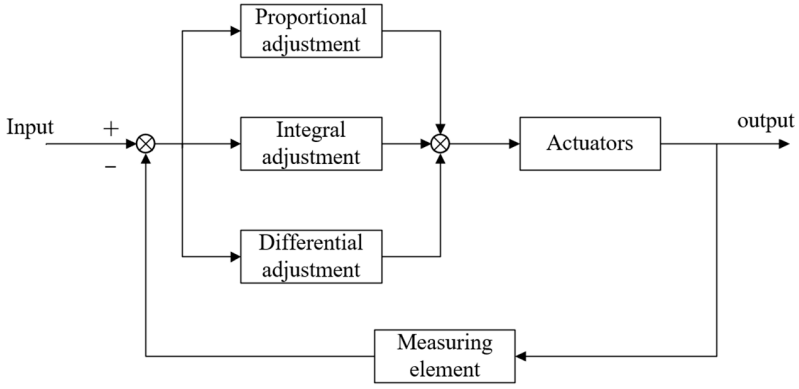


Figure 2. Principle of PID control algorithm.

Continuous control systems in industrial processes, generally using ideal PID control, have the following rules:

$$u(t) = K_p\left[e(t) + \frac{1}{T_I}\int_0^t e(t)dt + T_D\frac{de(t)}{dt}\right] \tag{1}$$

In Equation (1), $u(t)$ is the output signal of the PID controller, in this case the direction of motion and speed of the CNC guide. K_p is the proportionality factor, T_I is the integration time constant, T_D is the differentiation time constant and $e(t)$ is the difference between the input value and the actual value.

In many cases, when the control system is discrete, the control rule of the PID algorithm is:

$$u(k) = K_p e(k) + \frac{K_p T}{T_I}\sum_{n=0}^{k} e(n) + \frac{K_p T_D}{T}[e(k) - e(k-1)] \tag{2}$$

In Equation (2), $u(k)$ is the output signal at the k discrete time points, T is the two adjacent time intervals, and $e(k)$ is the difference between the given value and the measured value at the k discrete time points. For convenience, these coefficients are unified as follows:

$$u(k) = K_p e(k) + K_i\sum_{n=0}^{k} e(n) + K_d[e(k) - e(k-1)] \tag{3}$$

In Equation (3), the coefficients K_p, K_i, K_d need to be determined by trial and error in the experiment according to the characteristics of the system. The interface of the constant-force belt grinding test bench control software, written according to the PID algorithm, is shown in Figure 3. After connecting to the controller, set the required target pressure and grinding time and click on the "Start grinding" button to carry out constant force grinding according to the target pressure.

In order to test the effect of contact force control on the belt grinding test platform, the test pieces were ground at four combinations of target pressure of 5 N and 10 N and belt line speed of 10 m/s and 15 m/s respectively. According to the experimental results, the subject had a good results with contact pressure control at $[K_p, K_i, K_d] = [100, 3, 3]$, the time of The test experiment design table is shown in Table 2.

Table 2. Experiments to test the effect of contact pressure control.

Experiment No.	Belt Line Speeds (m/s)	Target Pressure (N)	K_p	K_i	K_d
1	10	5	100	3	3
2	10	10	100	3	3
3	15	5	100	3	3
4	15	10	100	3	3

Based on the pressure data recorded in real time, the actual contact pressure versus time was plotted as shown in Figure 4, which shows that the control software enables the test bench to perform constant force grinding.

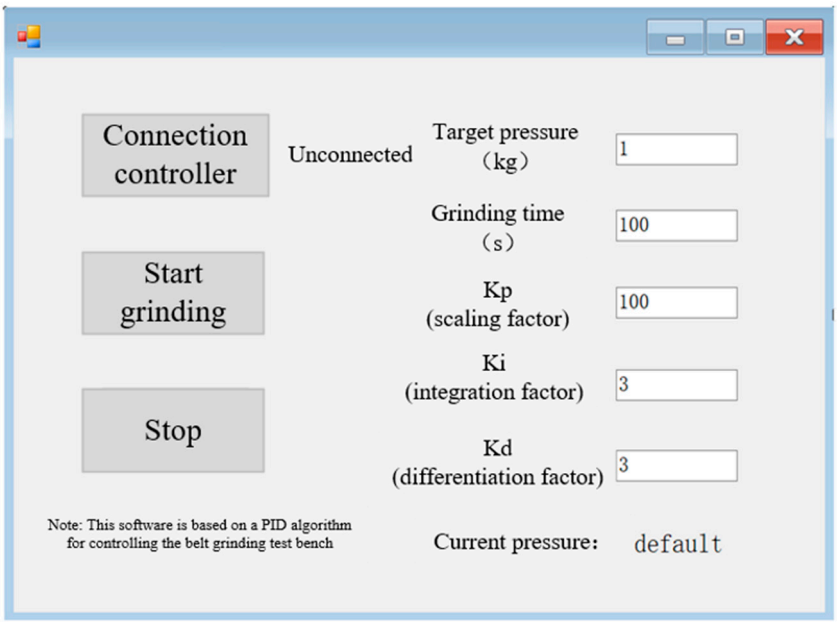


Figure 3. Control software for constant force belt grinding based on PID algorithm.

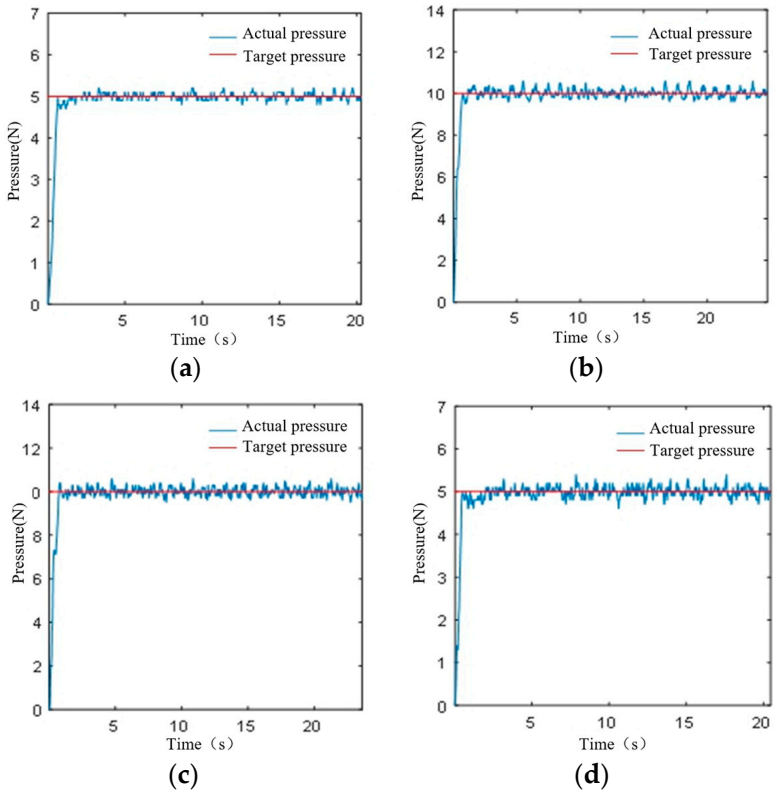


Figure 4. Variation of actual contact pressure versus time: (**a**) Target pressure 5 N, belt line speed 12 m/s; (**b**) Target pressure 5 N, belt line speed 16 m/s; (**c**) Target pressure 10 N, belt line speed 12 m/s; (**d**) Target pressure 10 N, belt line speed 16 m/s.

2.4. Test Programme

Firstly, the effects of abrasive particle size P, abrasive belt line speed Vs and grinding pressure F on the surface roughness were investigated through orthogonal tests; then, the unknowns in the theoretical model of surface roughness were calculated using the experimental data and the prediction model was tested for significance, and finally, the prediction model of surface roughness was validated.

The orthogonal test scheme is shown in Table 3 below. Using the orthogonal test can reduce the number of experiments and obtain the influence of the interaction of factors on the experimental index, and the L16 (three-factor four-level) orthogonal array model is selected in this paper.

Table 3. Orthogonal Experimental Design.

Factors / Horizontal	Abrasive Grain Size	Belt Line Speed (m/s)	Grinding Pressure (N)
1	80#	10	5
2	120#	15	10
3	150#	20	15
4	600#	25	20

3. Test Results and Analysis

3.1. Theoretical Modelling

The orthogonal test is useful for improving the accuracy of the theoretical model by studying the interaction effects between the factors. Therefore, this subject adopts a surface roughness prediction model based on the results of the orthogonal test. The theoretical empirical equation for the surface roughness Ra of abrasive belt grinding with abrasive grit P, belt line speed Vs and grinding pressure F can be expressed as [31]:

$$Ra = KP^{\alpha}V_s^{\beta}F^{\gamma} \tag{4}$$

In Equation (4), K is the scale factor and α, β and γ are the exponents of the corresponding parameters.

Equation (4) is a non-linear function, and taking the logarithm to linearize it gives:

$$\ln Ra = \ln k + \alpha \ln P + \beta \ln Vs + \gamma \ln F \tag{5}$$

Let Equation (5)

$$y = \ln Ra,\ x_1 = \ln P,\ x_2 = \ln Vs,\ x_3 = \ln F$$
$$a_0 = \ln k,\ a_1 = \alpha,\ a_2 = \beta,\ a_3 = \gamma$$

Then the corresponding linear regression Equation is:

$$y = a_0 + a_1x_1 + a_2x_2 + a_3x_3 \tag{6}$$

The equation contains three independent variables x_1, x_2, x_3 and the experimental results are expressed in terms of y. To calculate the values of a_0, a_1, a_2, a_3, total of 16 sets of orthogonal trials are conducted, where the experimental variables in group a_i are $x_{i1},\ x_{i2},\ x_{i3}$, and the corresponding trial results are y_i.

Let $\hat{a}_0, \hat{a}_1, \hat{a}_2, \hat{a}_3$ be the estimated vector of a_0, a_1, a_2, a_3 and $\hat{y}_i$ be the regression value of y_i. The regression Equation is $\hat{y}_i = \hat{a}_0 + \hat{a}_1x_{i1} + \hat{a}_2x_{i2} + \hat{a}_3x_{i3}$.

The difference between the experimental outcome value y_i and the regression value $\hat{y}_i$ is called the residual e_i, i.e., $e_i = y_i - \hat{y}_i = y_i - (\hat{a}_0 + \hat{a}_1x_{i1} + \hat{a}_2x_{i2} + \hat{a}_3x_{i3})$.

$\hat{a}_0, \hat{a}_1, \hat{a}_2, \hat{a}_3$ should be such that the sum of squares of e_i is minimized, i.e., to make:

$$\begin{aligned} Q &= (\hat{a}_0, \hat{a}_1, \hat{a}_2, \hat{a}_3) = \sum {e_i}^2 = \sum (y_i - \hat{y}_i)^2 \\ &= \sum (y_i - (\hat{a}_0 + \hat{a}_1 x_{i1} + \hat{a}_2 x_{i2} + \hat{a}_3 x_{i3}))^2 \end{aligned} \tag{7}$$

To obtain the minimum value for Q, find the partial derivatives of each variable of Q such that the derivative results in 0, i.e., $\frac{\partial Q}{\partial \hat{a}i} = 0 (i = 0, 1, 2, 3)$, denoted as:

$$\begin{cases} \frac{\partial Q}{\partial \hat{a}_0} = 2 \sum\limits_{i=1}^{16} (y_i - \hat{a}_0 - \hat{a}_1 x_{i1} - \hat{a}_2 x_{i2} - \hat{a}_3 x_{i3})(-1) = 0 \\ \frac{\partial Q}{\partial \hat{a}_1} = 2 \sum\limits_{i=1}^{16} (y_i - \hat{a}_0 - \hat{a}_1 x_{i1} - \hat{a}_2 x_{i2} - \hat{a}_3 x_{i3})(-x_{i1}) = 0 \\ \frac{\partial Q}{\partial \hat{a}_2} = 2 \sum\limits_{i=1}^{16} (y_i - \hat{a}_0 - \hat{a}_1 x_{i1} - \hat{a}_2 x_{i2} - \hat{a}_3 x_{i3})(-x_{i2}) = 0 \\ \frac{\partial Q}{\partial \hat{a}_3} = 2 \sum\limits_{i=1}^{16} (y_i - \hat{a}_0 - \hat{a}_1 x_{i1} - \hat{a}_2 x_{i2} - \hat{a}_3 x_{i3})(-x_{i3}) = 0 \end{cases}$$

The matrix form of the simplified system of Equations is expressed as:

$$\begin{bmatrix} 16 & \sum\limits_{i=1}^{16} x_{i1} & \sum\limits_{i=1}^{16} x_{i2} & \sum\limits_{i=1}^{16} x_{i3} \\ \sum\limits_{i=1}^{16} x_{i1} & \sum\limits_{i=1}^{16} {x_{i1}}^2 & \sum\limits_{i=1}^{16} x_{i1} x_{i2} & \sum\limits_{i=1}^{16} x_{i1} x_{i3} \\ \sum\limits_{i=1}^{16} x_{i2} & \sum\limits_{i=1}^{16} x_{i1} x_{i2} & \sum\limits_{i=1}^{16} {x_{i2}}^2 & \sum\limits_{i=1}^{16} x_{i2} x_{i3} \\ \sum\limits_{i=1}^{16} x_{i3} & \sum\limits_{i=1}^{16} x_{i1} x_{i3} & \sum\limits_{i=1}^{16} x_{i2} x_{i3} & \sum\limits_{i=1}^{16} {x_{i3}}^2 \end{bmatrix} \begin{bmatrix} \hat{a}_0 \\ \hat{a}_1 \\ \hat{a}_2 \\ \hat{a}_3 \end{bmatrix} = \begin{bmatrix} \sum\limits_{i=1}^{16} y_i \\ \sum\limits_{i=1}^{16} y_i x_{i1} \\ \sum\limits_{i=1}^{16} y_i x_{i2} \\ \sum\limits_{i=1}^{16} y_i x_{i3} \end{bmatrix}$$

This can be expressed in the form of $A \cdot B = C$

$$A = \begin{bmatrix} 1 & 1 & 1 & \dots & 1 \\ x_{11} & x_{21} & x_{31} & \dots & x_{161} \\ x_{12} & x_{22} & x_{32} & \dots & x_{162} \\ x_{13} & x_{23} & x_{33} & \dots & x_{163} \end{bmatrix} \begin{bmatrix} 1 & x_{11} & x_{12} & x_{13} \\ 1 & x_{21} & x_{22} & x_{23} \\ 1 & x_{31} & x_{32} & x_{33} \\ \dots & \dots & \dots & \dots \\ 1 & x_{161} & x_{162} & x_{163} \end{bmatrix}$$

$$B = \begin{bmatrix} \hat{a}_0 \\ \hat{a}_1 \\ \hat{a}_2 \\ \hat{a}_3 \end{bmatrix}, \; C = \begin{bmatrix} 1 & 1 & 1 & \dots & 1 \\ x_{11} & x_{21} & x_{31} & \dots & x_{161} \\ x_{12} & x_{22} & x_{32} & \dots & x_{162} \\ x_{13} & x_{23} & x_{33} & \dots & x_{163} \end{bmatrix} \begin{bmatrix} y_1 \\ y_2 \\ y_3 \\ \dots \\ y_{16} \end{bmatrix}$$

$$\text{Let } X = \begin{bmatrix} 1 & x_{11} & x_{12} & x_{13} \\ 1 & x_{21} & x_{22} & x_{23} \\ 1 & x_{31} & x_{32} & x_{33} \\ \dots & \dots & \dots & \dots \\ 1 & x_{161} & x_{162} & x_{163} \end{bmatrix}, \; Y = \begin{bmatrix} y_1 \\ y_2 \\ y_3 \\ \dots \\ y_{16} \end{bmatrix}, \; \hat{a} = \begin{bmatrix} \hat{a}_0 \\ \hat{a}_1 \\ \hat{a}_2 \\ \hat{a}_3 \end{bmatrix}$$

which in turn can be expressed as $X^T X \hat{a} = X^T Y$.

It can be derived that

$$\hat{a} = \left(X^T X \right)^{-1} X^T Y \tag{8}$$

The results of the orthogonal test are taken into Equation (8) to find the value of $\hat{a}$ and thus the specific expression of the surface roughness prediction model can be derived from Equation (6).

3.2. Orthogonal Tests and Analysis

In total, 16 sets of test data for the orthogonal test were obtained according to Table 2 and recorded in Table 4.

Table 4. Record of Orthogonal Test Results.

Serial No.	P	Vs	F	Ra	Serial No.	P	Vs	F	Ra
1	80#	10	5	0.863	9	150#	10	15	0.452
2	80#	15	10	0.662	10	150#	15	20	0.291
3	80#	20	15	0.573	11	150#	20	5	0.579
4	80#	25	20	0.423	12	150#	25	10	0.482
5	120#	10	10	0.491	13	600#	10	20	0.189
6	120#	15	5	0.715	14	600#	15	15	0.197
7	120#	20	20	0.402	15	600#	20	10	0.249
8	120#	25	15	0.469	16	600#	25	5	0.281

The results of the orthogonal tests were subjected to a polar difference analysis to derive the level of influence on the surface roughness of each factor and the results of the polar difference analysis are shown in Table 5.

Table 5. Table of Extreme Difference Analysis.

Factors	Abrasive Grain Size	Belt Line Speed	Grinding Pressure
K1	0.630	0.499	0.610
K2	0.519	0.466	0.471
K3	0.451	0.451	0.423
K4	0.229	0.414	0.326
Extreme difference R	0.401	0.085	0.284

From the extreme difference analysis, it can be seen that surface roughness is most influenced by abrasive grit size, followed by grinding pressure, and least influenced by belt line speed. The surface roughness decreases with increasing abrasive grit size, decreases with increasing belt line speed and decreases with increasing grinding pressure.

Meanwhile, according to the analysis in Table 5, it can be seen that the surface roughness ($Ra = 0.229$ μm) is the lowest among the four levels when the belt grit size is selected at level 4 (600#); the surface roughness ($Ra = 0.414$ μm) is the lowest among the four levels when the belt line speed is selected at level 4 (25 m/s); the surface roughness ($Ra = 0.326$ μm) is the lowest among the four levels. Therefore, when the belt grit size is 600#, the belt line speed is 25 m/s and the grinding pressure is 20 N, the surface roughness is the better combination of the machining parameters.

3.3. Theoretical Model Calculations

The expressions in the theoretical model are calculated from the surface roughness test data in the orthogonal test results in Table 4, and the logarithmic table corresponding to the test results is shown in Table 6 below.

$$\text{It is obtained that } \hat{a} = \begin{bmatrix} \hat{a}_0 \\ \hat{a}_1 \\ \hat{a}_2 \\ \hat{a}_3 \end{bmatrix} = \begin{bmatrix} 2.8039 \\ -0.4943 \\ -0.0595 \\ -0.4018 \end{bmatrix} \tag{9}$$

The regression Equation is determined from Equation (6) as:

$$\begin{aligned} y &= a_0 + a_1 x_1 + a_2 x_2 + a_3 x_3 \\ &= 2.8039 - 0.4943 x_1 - 0.0595 x_2 - 0.4018 x_3 \end{aligned}$$

Table 6. Logarithm of Orthogonal Experimental Results.

Serial No.	$x_{i1}(lnP)$	$x_{i2}(\ln Vs)$	$x_{i3}(lnF)$	$y_i(lnRa)$
1	4.3820	2.3026	1.6094	−0.1472
2	4.3820	2.7081	2.3026	−0.4120
3	4.3820	2.9957	2.7081	−0.5567
4	4.3820	3.2189	2.9957	−0.8599
5	4.7875	2.3026	2.3026	−0.7111
6	4.7875	2.7081	1.6094	−0.3358
7	4.7875	2.9957	2.9957	−0.9111
8	4.7875	3.2189	2.7081	−0.7574
9	5.0106	2.3026	2.9957	−0.7936
10	5.0106	2.7081	1.6094	−1.2334
11	5.0106	2.9957	2.3026	−0.5473
12	5.0106	3.2189	2.7081	−0.7292
13	6.3969	2.3026	2.9957	−1.6650
14	6.3969	2.7081	2.7081	−1.6261
15	6.3969	2.9957	2.3026	−1.3899
16	6.3969	3.2189	1.6094	−1.2698

Since $a_0 = lnK,\ K = 16.5089$, The final model for predicting the surface roughness of titanium alloy for abrasive belt grinding is obtained as:

$$Ra = 16.5089P^{-0.4943}Vs^{-0.0595}F^{-0.4018} \tag{10}$$

3.4. Significance Tests of the Predictive Model

3.4.1. Significance Tests of the Regression Equations

The squared values of the correlation coefficients and the values of the ANOVA significance probabilities were calculated using MATLAB R2021b (MathWorks Inc., Natick, MA, USA).

$$R^2 = 0.9282,\ P = 0.0000\ 0423$$

where R denotes the linearity of the linear regression equation. Generally, a correlation coefficient with an absolute value in the range of 0.8 to 1 indicates a strong linearity of the regression equation. This shows that the linear correlation of the prediction model is strong.

The errors in the test results are mainly due to two factors, namely the different values of the influencing factors, random errors due to measurements, etc., or the influence of other factors. Therefore, in order to determine whether the prediction model can accurately fit the results, the prediction model needs to be tested for significance.

$$\text{It is obtained that} \begin{cases} S_A = \sum_{i=1}^{n} (\hat{y}_i - \overline{y})^2 \\ S_T = \sum_{i=1}^{n} (y_i - \overline{y})^2 \\ S_E = \sum_{i=1}^{n} (y_i - \hat{y}_i)^2 \\ S_T = S_A + S_E \end{cases} \tag{11}$$

and S_A and S_E are independent of each other. where y_i is the roughness value obtained from the test; $\overline{y}$ is the average of the measured values; and $\hat{y}_i$ is the calculated value of the prediction formula.

According to Equation (11), $S_T = 0.5491, S_E = 0.0169$ and $S_A = 0.5322$

$$F = \frac{S_A/m}{S_E/n-m-1} \sim F(m, n-m-1) \tag{12}$$

In Equation (12): n is the number of experimental groups, $n = 16$; m is the number of variables, $m = 3$.

$F = 126.3171$ was obtained, and when the test significance level was taken as $\alpha = 0.05$, it can be seen from the table that $F_{0.05}(3, 12) = 3.49$, which is smaller than the calculated F value, so the regression equation is significant; the ANOVA significance probability value $P = 0.0000333$ is less than 0.05, and the regression equation is significant; as shown in Figure 5, it is the regression equation residual analysis graph, in which the dot is the data residual. As shown in Figure 5, the residuals of the regression equation are the data residuals and the line segment is the confidence interval.

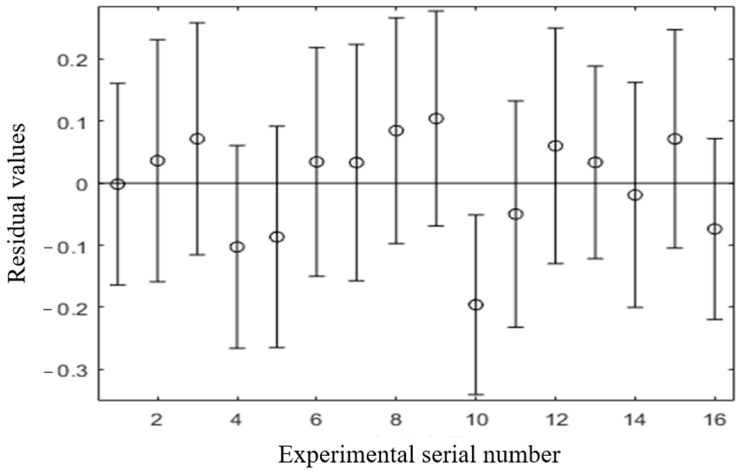


Figure 5. Residual Analysis of the Regression Equation.

3.4.2. Significance Tests of the Regression Coefficients

The significance of the regression equation does not indicate that the independent variables in the equation are significant, so significance tests are carried out on the coefficients in the regression equation to determine the significance of each process parameter on the surface roughness. For hypothesis $H_{\alpha i} : \beta_i = 0$, the following statistic was used:

$$F_i = \frac{\hat{a}_i^2 / C_{ii}}{S_E / (n - m - 1)} \sim F(1, n - m - 1) \tag{13}$$

In Equation (13) C_{ii} is the corresponding diagonal element in matrix $C = (X^T X)^{-1}$ and $\hat{a}_i$ is the corresponding coefficient.

$$C = \begin{bmatrix} 1.066867 & -0.000334 & -0.035 & -0.025 \\ -0.000334 & 0.000001 & 0 & 0 \\ -0.035 & 0 & 0.002 & 0 \\ -0.025 & 0 & 0 & 0.002 \end{bmatrix}$$

Checking the table, we find $F_{0.05}(1, 12) = 4.7472$. The regression coefficients calculated from Equation (13) are shown in Table 7 below.

Table 7. Results of regression coefficient calculation.

Regression Coefficient	a_0	a_1	a_2	a_3
Fi	5247.16	123,645,071.80	1260.41	57,477.67
Significance		$a_1 > a_3 > a_0 > a_2 > 4.7472$		

It can be seen that a_0, a_1, a_2 and a_3 are all significant, meaning that in abrasive belt grinding processes, the surface roughness is greatly influenced by the abrasive grit, belt line speed and grinding pressure.

4. Validation of the Predictive Model

Relying on the grinding test bench built in Section 2.2, a series of grinding experiments were designed to investigate the influence of the key machining parameters identified in Chapter 2 on the surface roughness. The test pieces, abrasive belts and other experimental parameters used are as follows.

Specimen parameters: material: bar stock of TC4 titanium alloy, size: 15 mm × 40 mm (diameter × length).

Belt parameters: abrasive material: aluminum oxide; belt width: W = 25 mm; belt circumference: L = 1510 mm. The four types of abrasive belts used are shown in Figure 6 below, from left to right, 80#, 120#, 150# and 600#.

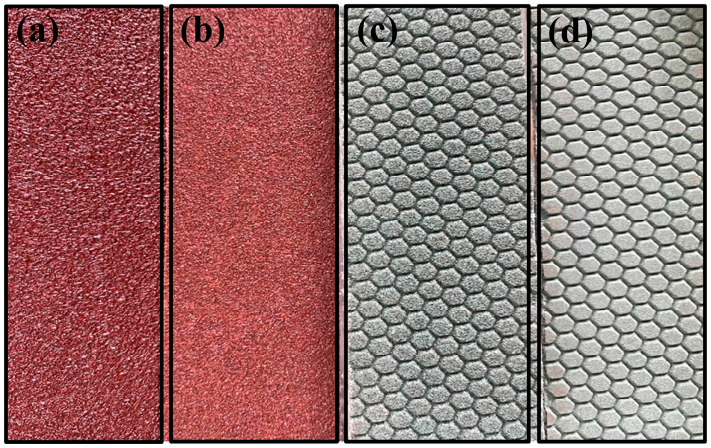


Figure 6. Four different types of abrasive belts. From left to right, they are (**a**) 80#, (**b**) 120#, (**c**) 150#, (**d**) 600#.

Contact wheel parameters: hub material: aluminum alloy; outer ring material: rubber; diameter: 200 mm; thickness: 25 mm.

Belt sander parameters: rated power: 1500 W, maximum motor speed: 2800 r/min.

Parameters of the CNC guide: Repeat positioning accuracy: 0.55 mm, maximum horizontal load: 25 kg, maximum vertical load: 15 kg, horizontal full load speed: 80 mm/s, maximum thrust: 471 N.

Pressure sensor parameters: range: 50 kg, measuring accuracy: 0.1%, sensitivity: 1.5 ± 10% mV/V.

Surface roughness is measured using the ZeGage™ (ZYGO Corporation, Middlefield, CT, USA). The non-contact measurement method of the ZeGage™ optical profiler is used to quantify the three-dimensional shape of the workpiece and measure the surface roughness. The high-resolution graphic sensor enables fast measurements in a matter of seconds and gives excellent imaging of surface details [32].

From the various indices in regression Equation (7), it can be seen that the factor that has the greatest effect on blade belt grinding is abrasive grit size, followed by grinding pressure and belt line speed.

The results of the orthogonal experiment, Table 3, were taken into Equation (7) to produce predicted values of surface roughness and the relative error between the experimental and predicted values was calculated, as shown in Table 8 below.

Figure 7 shows the comparison between the experimental and predicted values of surface roughness. It can be seen that the relative errors of surface roughness for numbers 4 and 10 are large, 10.8% and 21.62%, respectively. Overall, the surface roughness prediction model established is in good agreement with the experimental values. The relative errors in surface roughness for experiment numbers 1 and 14 were smaller, at 0.14% and 1.89%, respectively.

Table 8. Surface Roughness Prediction Grinding Verification.

Serial No.	Experimental Values	Predicted Value	Relative Error	Serial No.	Experimental Values	Experimental Values	Relative Error
1	0.863	0.864	0.14%	9	0.452	0.407	−9.91%
2	0.662	0.639	−3.58%	10	0.291	0.354	21.62%
3	0.573	0.533	−6.93%	11	0.579	0.608	5.08%
4	0.423	0.469	10.8%	12	0.482	0.454	−5.86%
5	0.491	0.535	9.02%	13	0.189	0.183	−3.33%
6	0.715	0.690	−3.40%	14	0.197	0.200	1.89%
7	0.402	0.389	−3.29%	15	0.249	0.232	−6.91%
8	0.469	0.431	−8.13%	16	0.281	0.302	7.62%

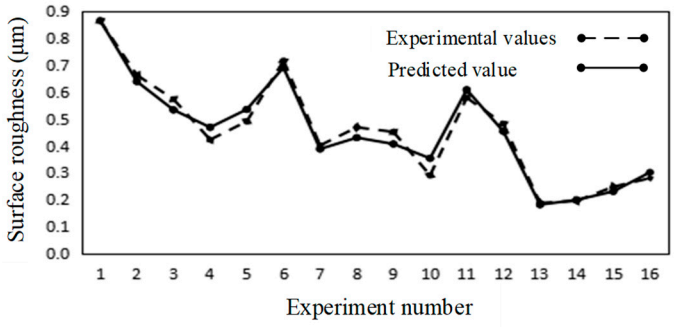


Figure 7. Comparison of Predicted Surface Roughness and Experimental Values.

A randomized test was used to validate the theoretical roughness model. The same test equipment material was selected and the test was carried out. The surface roughness was measured and the error between the test and predicted values was calculated and analyzed. The results of the random test are shown in Table 8, where Ra denotes the measured value of surface roughness, Ra^* denotes the predicted value of roughness, E denotes the relative error and the calculation formula is $E = \frac{Ra^* - Ra}{Ra}$.

As can be seen from Table 9, there are certain errors between the measured values and the predicted values in the eight sets of random tests, and the errors are all less than 10%, indicating that the surface roughness prediction model has certain reliability and accuracy. Therefore, the prediction model can be used to adjust the process parameters in the grinding process to achieve the role of controlling and predicting the surface roughness of the workpiece, which has important practical application value.

Table 9. Table of Results of Randomized Trials.

Serial No.	P	Vs	F	Ra	Ra*	E
1	80#	8	3	1.133	1.075	−5.08%
2	150#	8	25	0.308	0.336	9.17%
3	120#	30	2	1.027	0.957	−6.77%
4	600#	30	25	0.171	0.157	−8.40%
5	150#	19	14	0.399	0.403	1.04%
6	80#	23	9	0.604	0.650	7.53%
7	120#	12	18	0.453	0.418	−7.68%
8	600#	20	12	0.224	0.216	−3.79%

5. Test Validation

5.1. Selection of Experimental Grinding Process Parameters

The experimental workpiece is a certain type of aeronautical blade, the blade material is TC4, the abrasive belt and contact wheel are the same as those mentioned in Section 4. The tool walking method is selected for longitudinal grinding, with the abrasive belt rotating at high speed and the workpiece making a circular feeding motion, with the table reciprocating vertically for a linear feeding motion, creating a parallel and effective space at

the front end of the abrasive belt in which the abrasive grains and the workpiece material move relative to each other, thus achieving automatic removal of the metal chips. During belt grinding, the contact area between the abrasive belt and the blade is smaller, which avoids the rippling phenomenon along the belt direction and can effectively reduce the damage to the surface of the component with high machining accuracy and surface quality and adaptability [33].

The purpose of this experiment is twofold: one is to verify the accuracy of the surface roughness prediction model, and the other is to verify the correctness of the parameter combination preferences, considering only the influence produced by the experimental material and processing parameters. Therefore, the process parameters selected are shown in Table 10 below.

Table 10. Experimental process parameters.

Serial No.	Abrasive Grain Size	Belt Line Speed (m/s)	Grinding Pressure (*N*)
1	80#	20	15
2	80#	10	5
3	80#	15	10
4	120#	20	20
5	120#	15	5
6	120#	10	5
7	600#	10	20
8	600#	20	10
9	600#	25	5

5.2. Analysis of Surface Roughness

According to the surface roughness prediction formula, Equation (10), the parameters in Table 10 are brought into it and the corresponding predicted values are calculated to determine the correct choice of parameter combinations, and the predicted values are compared with the calculated values as shown in Table 11 below.

Table 11. Validation of experimental results.

Serial No.	Experimental Values	Predicted Value	Relative Error	Corresponding Parameter Range
1	0.594	0.533	−10.20%	0.50–0.63
2	0.360	0.342	5.01%	0.30–0.40
3	0.476	0.451	5.31%	0.47–0.50
4	0.417	0.389	−6.74%	0.40–0.50
5	0.758	0.690	−8.91%	0.63–1.00
6	0.611	0.653	6.87%	0.60–0.65
7	0.169	0.183	8.23%	0.16–0.20
8	0.237	0.232	−2.16%	0.20–0.25
9	0.283	0.302	6.82%	0.25–0.32

According to the experimental results, it can be seen that the maximum error of the prediction model is 10.2%, which proves that the prediction model has a good predictive effect to a certain extent, and the selected parameter combinations are in line with the corresponding surface roughness range, which proves that the selection of parameter combinations also has a certain degree of reliability. By relying on the combination of parameters and prediction models, a certain guiding role can be achieved for grinding processing. Setting reasonable process parameters can lead to obtaining the ideal grinding surface.

5.3. Analysis of Surface Micromorphological

In the field of machining, none of the surfaces obtained by machining methods is an ideal finish, and the surfaces produced by different machining methods vary. The microscopic shape of the surface of a workpiece is formed gradually during the machining

process and is sensitive to changes in the process, with variations in the parameters causing differences in the surface shape. Therefore, the study of surface morphology helps to better understand the condition of the whole workpiece and the extent to which different parameters affect the workpiece.

The most representative six of the nine groups of experiments carried out according to Table 10 were selected for surface microform analysis, as shown in Figure 8. The surface micromorphology is shown in Figure 9 for the finish milling process carried out prior to grinding, all at a magnification of 200×.

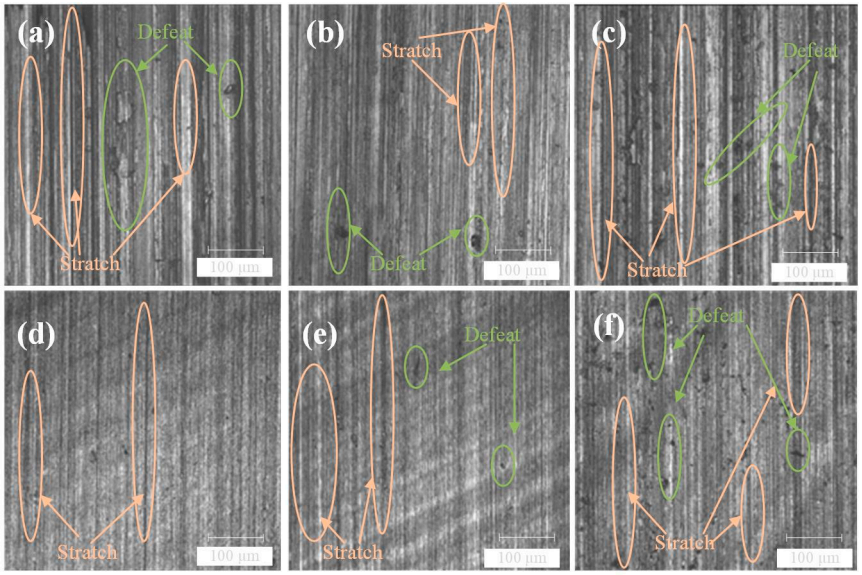


Figure 8. This is microscopic morphology of the abrasive belt grinding surface of the blade: (**a**) #80, 20 m/s, 15 N; (**b**) #120, 20 m/s, 20 N; (**c**) #120, 15 m/s, 5 N; (**d**) #600, 10 m/s, 20 N; (**e**) #600, 20 m/s, 10 N; (**f**) #600, 25 m/s, 5 N.

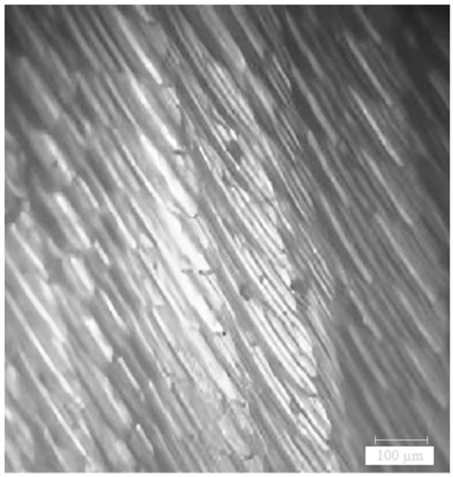


Figure 9. Microscopic view of the finely milled surface of the blade.

As can be seen from Figure 9, the surface texture machined by fine milling is relatively neat, with balanced spacing and a certain degree of directionality, but the surface roughness is high and there are local faults. After the grinding process, as the abrasive grain size changes from coarse to fine, the grinding texture also changes from coarse to fine accordingly, reflecting the difference in abrasive grain size, and is also influenced by a certain grinding pressure and belt line speed. During the grinding process, water cooling was used and the cooling was adequate; no obvious burn marks appeared on the surface. The microscopic morphology of Figure 8d shows the uniformity of the abrasion marks

and the clear surface texture after grinding. The average roughness value of the machined surface of TC4 titanium alloy is 0.23 μm, which is nearly five times lower compared to the original surface. The surface microstructure shows that the defects are significantly reduced and the surface quality is improved.

The analysis of the grinding profile of TC4 titanium alloy blades further validates the accuracy and effectiveness of the key process parameters determined using roughness set theory and hierarchical analysis. Although the surface profile only reflects the surface geometry and surface characteristics, it also has an important influence on the wear resistance, corrosion resistance and fatigue life of the material. The reasonableness and feasibility of using abrasive belt grinding to grind the surface of TC4 titanium alloy is also verified.

6. Conclusions and Perspectives

Unlike conventional grinding process methods, which rely on operator experience, this paper establishes a model for predicting the accuracy of surface roughness of titanium alloys in abrasive belt machining, and the following conclusions are obtained from the experimental results:

1. In abrasive belt grinding of titanium alloy surfaces, experiments were carried out using elastic grinding on workpiece surfaces with different abrasive grit sizes, feed rates and grinding pressures. The results show that when grinding the workpiece surface, the process factor that has the greatest influence on the machined surface roughness is the abrasive grit, followed by the grinding pressure. The abrasive belt line speed has the least influence. The optimum level of grinding parameters is $A_4B_4C_4$, i.e., abrasive grit size of 600#, belt line speed of 25 m/s and grinding pressure of 20 N.
2. The interaction effects between the experimental data and various factors such as abrasive particle size P and abrasive belt line speed Vs were summarized. On this basis, the experimental data were analyzed and complex mathematical modelling was carried out to establish a surface roughness prediction model, and the mathematical expression $Ra = 16.5089P^{-0.4943} - 0.4943Vs^{-0.0595} - 0.0595F^{-0.4018}$ for the prediction model of surface roughness of titanium alloy by abrasive belt grinding was obtained.
3. A series of grinding experiments on titanium alloy, verification of the preferential selection of parameter combinations and comparison with the surface roughness prediction model show that the roughness of the ground surface is in high agreement with the prediction results, and the minimum relative error achieved by the prediction model is 2.16% and the maximum relative error is 10.2%, indicating that the prediction model has a certain degree of accuracy, and the selection of a reasonable combination of parameters and the combination of the prediction model to adjust them. The selection of a reasonable combination of parameters and the corresponding adjustment of the parameters in combination with the prediction model can obtain workpieces that meet the requirements, which has certain guiding significance for the actual grinding process.

Author Contributions: Conceptualization, H.Q. and Y.X.; original draft preparation, H.Q. and S.H.; methodology and formal analysis, H.Q., S.H., Y.X., S.L. and L.Z.; validation and formal analysis, H.Q., S.H., Y.X., S.L. and L.Z.; supervision, H.Q., Y.X., S.L. and L.Z.; All authors have read and agreed to the published version of the manuscript.

Funding: This research was funded by the Shaanxi Science and Technology Resources Open Sharing Platform (Project No.: 2021PT-006), the Shaanxi Innovative Talent Promotion Plan—Science and Technology Innovation Team (Project No.: 2018TD-036), Shaanxi International Science and Technology Cooperation Base (Project No.: 2022GHJD-14), Shaanxi General Projects—Social Development Area (Project No.: 2019SF-262).

Data Availability Statement: Not applicable.

Conflicts of Interest: The authors declare no conflict of interest.

References

1. Shen, X.; Zhang, D.; Yao, C.; Tan, L. Research progress on the mechanism of surface integrity formation in titanium alloy cutting. *J. Aerosp. Mater.* **2021**, *41*, 1–16.
2. Wu, Q. Basic Research on the Deformation of Thin-Walled Blade Milling of High Temperature Alloys. Master's Thesis, The Nanjing University of Aeronautics and Astronautics, Nanjing, China, 2016.
3. Klocke, F.; Herrig, T.; Zeis, M.; Klink, A. Comparison of the electrochemical machinability of electron beam melted and casted gamma titanium aluminide TNB-V5. *Proc. Inst. Mech. Eng. Part B J. Eng. Manuf.* **2018**, *232*, 586–592. [CrossRef]
4. Sun, J.; Huang, S.; Wang, T.; Chen, W. Research on surface integrity of turning titanium alloy TB6. *Procedia CIRP* **2018**, *71*, 484–489. [CrossRef]
5. Guo, S.; Lu, S.; Zhang, B.; Cheung, C.F. Surface integrity and material removal mechanisms in high-speed grinding of Al/SiCp metal matrix composites. *Int. J. Mach. Tools Manuf.* **2022**, *178*, 103906. [CrossRef]
6. M'Saoubi, R.; Axinte, D.; Soo, S.L.; Nobel, C.; Attia, H.; Kappmeyer, G.; Engin, S.; Sim, W.-M. High performance cutting of advanced aerospace alloys and composite materials. *CIRP Ann.* **2015**, *64*, 557–580. [CrossRef]
7. Wu, Z.; Kou, H.; Chen, N.; Xi, Z.; Fan, J.; Tang, B.; Li, J. Recent developments in cold dwell fatigue of titanium alloys for aero-engine applications: A review. *J. Mater. Res. Technol.* **2022**, *20*, 469–484. [CrossRef]
8. Zhang, X.; Chen, Y.; Hu, J. Recent advances in the development of aerospace materials. *Prog. Aerosp. Sci.* **2018**, *97*, 22–34. [CrossRef]
9. Yang, J.; Wang, X.; Kang, M. Finite Element Simulation of Surface Roughness in Diamond Turning of Spherical Surfaces. *J. Manuf. Process.* **2018**, *31*, 768–775. [CrossRef]
10. Zhang, S.; Yang, Z.; Jiang, R.; Jin, Q.; Zhang, Q.; Wang, W. Effect of creep feed grinding on surface integrity and fatigue life of Ni3Al based superalloy IC10. Chin. *J. Aeronaut.* **2021**, *34*, 438–448. [CrossRef]
11. Luo, G.; Zou, L.; Huang, Y.; Gong, M. Study on material removal and surface quality of titanium alloy by abrasive belt grinding of alumina hollow spheres. *China Mech. Eng.* **2020**, *31*, 2363–2370.
12. Wu, X.-J.; Yang, Y.; Tong, X.; Shu, X.; Li, Y. The Grey Theory Combining the Taguchi Method for the Best Parameters: A Case Study of Polishing M300 Steel. *Math. Probl. Eng.* **2019**, *2019*, 1–13. [CrossRef]
13. Zhang, J.-J.; Liu, J.; Yang, S.-Q.; Li, J.-Z. Optimized prediction model and experimental study on surface roughness of blade polishing. *Mech. Des. Manuf.* **2021**, *12*, 1–5.
14. Gopal, A.V.; Rao, P.V. Selection of optimum conditions for maximum material removal rate with surface finish and damage as constraints in SiC grinding. *Int. J. Mach. Tools Manuf.* **2003**, *43*, 1327–1336. [CrossRef]
15. Yusup, N.; Zain, A.M.; Hashim, S.Z.M. Evolutionary techniques in optimizing machining parameters: Review and recent applications (2007–2011). *Exp. Syst. Appl.* **2012**, *39*, 9909–9927. [CrossRef]
16. Rao, R.V.; Rai, D.P.; Balic, J. A multi-objective algorithm for optimization of modern machining processes. *Eng. Appl. Artif. Intell.* **2017**, *61*, 103–125. [CrossRef]
17. Patil, P.J.; Patil, C.R. Analysis of process parameters in surface grinding using single objective Taguchi and multi-objective grey relational grade. *Perspect. Sci.* **2016**, *8*, 367–369. [CrossRef]
18. Nee, C.Y.; Saad, M.S.; Nor, A.M.; Zakaria, M.Z.; Baharudin, M.E. Optimal process parameters for minimizing the surface roughness in CNC lathe machining of Co28Cr6Mo medical alloy using differential evolution. *Int. J. Adv. Manuf. Technol.* **2018**, *97*, 1541–1555. [CrossRef]
19. Neşeli, S.; Asiltürk, I.; Çelik, L. Determining the optimum process parameter for grinding operations using robust process. *J. Mech. Sci. Technol.* **2012**, *26*, 3587–3595. [CrossRef]
20. de Souza Ruzzi, R.; da Silva, R.B.; da Silva, L.R.R.; Machado, Á.R.; Jackson, M.J.; Hassui, A. Influence of grinding parameters on Inconel 625 surface grinding. *J. Manuf. Process.* **2020**, *55*, 174–185. [CrossRef]
21. Wei, G.; Yang, S.; Tian, J.; Yang, Y.; Fan, X.; Wei, W. Research on the Optimization Model of the Abrasive Blocks Using Weighted Case-Based Reasoning. *Math. Probl. Eng.* **2019**, *2019*, 1–12.
22. Zhang, H.; Li, C.; Yao, G.; Shi, Y.; Zhang, Y. Investigation of surface quality, microstructure, deformation mechanism, and fatigue performance of additively manufactured 304 L stainless steel using grinding. *Int. J. Fatigue* **2022**, *160*, 106838. [CrossRef]
23. Khodaii, J.; Adibi, H.; Barazandeh, F.; Rezaei, M.; Sarhan, A.A. Investigation of the surface integrity, flexural strength on the grinding of alumina for biomedical applications. *Precis. Eng.* **2021**, *67*, 110–122. [CrossRef]
24. Furno, M.E.; Sosa, A.D. Surface integrity analysis of grinding on ductile iron. *Int. J. Adv. Manuf. Technol.* **2020**, *110*, 2067–2078. [CrossRef]
25. Vendrame, S.; da Silva, R.B.; Machado, Á.R.; Bianchi, E.C.; Aguiar, P.R.; Baptista, F.G.; de Angelo Sanchez, L.E.; Jackson, M.J. Surface integrity assessment of M3 HSS cutting taps after grinding at various machining conditions. *Int. J. Adv. Manuf. Technol.* **2018**, *98*, 617–627. [CrossRef]
26. Wang, T.; Zou, L.; Wan, Q.; Zhang, X.; Li, Y.; Huang, Y. A high-precision prediction model of surface roughness in abrasive belt flexible grinding of aero-engine blade. *J. Manuf. Process.* **2021**, *66*, 364–375. [CrossRef]
27. He, Z.; Li, J.Y.; Liu, Y.M.; Nie, M.; Fan, W.G. Investigating the effects of contact pressure onrail material abrasive belt grinding performance. *Int. J. Adv. Manuf. Tech.* **2017**, *93*, 779–786.
28. Guo, Z.; Yu, H.; Chen, L. High-speed galvanometer motor control based on fuzzy PID. *Small Spec. Electr. Mach.* **2019**, *47*, 1–5.

29. Astrom, K.J.; Wittenmark, B. Self-tuning controllers based on pole-zero placement. *IEE Proc. D-Control. Theory Appl.* **1980**, *127*, 120–130. [CrossRef]
30. Zhou, J.; Gan, Y.F. *Computer Control Technology*; Nanjing Southeast University Press: Nanjing, China, 2016.
31. Ye, X. *Research on Surface Integrity of CNC Abrasive Belt Grinding of Aero-Engineered Titanium Alloy Blades*; Chongqing University: Chongqing, China, 2013.
32. Liu, P.-Z.; Zou, W.-J.; Peng, J.; Song, X.-D.; Xiao, F.-R. Study on the effect of grinding pressure on material removal behavior performed on a self-designed passive grinding simulator. *Appl. Sci.* **2021**, *11*, 4128. [CrossRef]
33. He, Z.; Li, J.Y.; Liu, Y.M.; Yan, J.W. Investigation on wear modes and mechanisms of abrasive belts in grinding of U71Mn steel. *Int. J. Adv. Manuf. Tech.* **2019**, *101*, 1821–1835. [CrossRef]

Disclaimer/Publisher's Note: The statements, opinions and data contained in all publications are solely those of the individual author(s) and contributor(s) and not of MDPI and/or the editor(s). MDPI and/or the editor(s) disclaim responsibility for any injury to people or property resulting from any ideas, methods, instructions or products referred to in the content.